A New VLSI 2-D Fourfold-Rotational-Symmetry Filter Architecture Design

Pei-Yu Chen, Lan-Da Van
Department of Computer Science,
National Chiao Tung University,
Hsinchu, Taiwan
e-mail: ldvan@cs.nctu.edu.tw

Hari C. Reddy, *Fellow of IEEE,*
Department of Elecrical Engineering,
California State University, Long Beach, USA and National Chiao Tung University, Hsinchu, Taiwan
e-mail: hreddy@csulb.edu

Chin-Teng Lin, *Fellow of IEEE,*
Department of Computer Science,
National Chiao Tung University,
Hsinchu, Taiwan
e-mail: ctlin@mail.nctu.edu.tw

Abstract—**In this paper, we propose two new two-dimensional (2-D) IIR and FIR filter architectures for 2-D transfer function using fourfold rotational symmetry. The presented type-I structure with fourfold rotational symmetry has the lowest number of multipliers, and zero latency. Importantly, the proposed type-II IIR filter possesses high speed, local broadcast, and the same number of multipliers and latency as the type I shows at expense of a slight increment of number of delay elements.**

INTRODUCTION

Recently, 2-D digital filters are widely applied in a variety of digital signal processing (DSP) systems such as image restoration [1] obtained through a 2-D low-pass intraframe filter, image enhancement [2, 3] performed by a 2-D high-pass filter and bio-medical signal processing [4]. Several 2-D filter VLSI architectures have been existed in [7-11], and an existing ASIC approach has been applied to design 2-D diagonal symmetry transfer function [12]. However, the VLSI architecture and hardware evaluation metrics using other frequency symmetry have not been discussed. Thus, we are motivated to propose one new 2-D IIR and FIR filter with less number of multipliers using fourfold rotational symmetry property [5, 6]. The comparison results among the structures of [8, 10. 11] and the proposed one in terms of hardware evaluation metrics are also debated in this paper. Note that when the frequency response has no symmetry, there is a technique to decompose that frequency response into components each of which has the desired symmetry. As a consequence, there is a motivation to derive the 2-D fourfold-rotational-symmetry IIR and FIR filter architecture designs.

The structure of this paper is organized as follows. The brief review of fourfold rotational symmetries is presented in Section II. The proposed 2-D fourfold-rotational-symmetry IIR and FIR filter architectures are discussed in Section III. In Section IV, the comparison results are tabulated in terms of the number of multipliers, critical period, latency, and whether the local broadcast exists. In the last section, concise statements conclude this presentation.

This work was supported in part by the National Science Council (NSC) Grant NSC-96-2220-E-009-038, NSC-97-2220-E-009-055, and MOEA-96-EC-17-A-01-S1-048.

REVIW OF FOURFOLD ROTATIONAL SYMMETRY

2-D frequency responses possess many types of symmetries and the presence of these symmetries can be used to reduce the design complexity of these filters. Symmetry in a frequency response induces certain constraints on the coefficients of filter transfer function which in turn reduces the filter design complexity. In the following, the fourfold rotational symmetry constraints on polynomials are reviewed.

For a 2-D z-domain polynomial $Q(z_1, z_2)$, we can represent the magnitude squared function of the frequency response in the form

$$F(\theta_1,\theta_2) = Q(e^{j\theta_1}, e^{j\theta_2}) \cdot Q^*(e^{-j\theta_1}, e^{-j\theta_2})$$
$$= Q(z_1, z_2) \cdot Q^*(z_1^{-1}, z_2^{-1})\,|_{z_i = z^{j\theta_i}}\ , for\ i = 1, 2 \qquad (1)$$

Where Q^* is obtained by complex conjugating the coefficients of Q. A magnitude squared function of the frequency response with fourfold rotational symmetry can be defined as

$$F(\theta_1,\theta_2) = F(-\theta_2,\theta_1)$$
$$= F(-\theta_1,-\theta_2) = F(\theta_2,-\theta_1) \quad ,\forall(\theta_1,\theta_2) \qquad (2)$$

Since real polynomials always satisfy $F(\theta_1, \theta_2) = F(-\theta_1, -\theta_2)$, $F(\theta_1, \theta_2) = F(-\theta_2, \theta_1)$ is enough to ensure the fourfold rotational symmetry. Using the magnitude squared function in (1) and fourfold rotational symmetry definition in (2), we can conclude the following factors [5] with fourfold rotational symmetry in their magnitude responses:

$$Factor1 = Q_1(x_1, x_2) + y_1 y_2 \cdot (x_1 - x_2) \cdot Q_2(x_1, x_2) \qquad (3a)$$

$$Factor2 = (x_1 - x_2) Q_1(x_1, x_2) + y_1 y_2 Q_2(x_1, x_2) \qquad (3b)$$

$$Factor3 = Q(z_1, z_2) \cdot Q(z_2^{-1}, z_1) \qquad (3c)$$

$$Factor4 = Q(z_1, z_2) \cdot Q(z_2, z_1^{-1}) \qquad (3d)$$

$$Factor5 = Q(z_1, z_2) \cdot Q(z_2^{-1}, z_1) \cdot Q(z_1^{-1}, z_2^{-1}) \cdot Q(z_2, z_1^{-1}) \qquad (3e)$$

Where $Q_k(x_1,x_2)=Q_k(x_2,x_1)$ for k =1, 2, and $x_i=z_i+z_i^{-1}$, $y_i=z_i-z_i^{-1}$ for i=1, 2.

Using the fourfold rotational symmetry constraints on polynomial factors, a procedure to design a 2-D IIR and FIR digital filter architectures is presented in the next section.

2-D FOURFOLD-ROTATIONAL SYMMETRY DIGITAL FILTER ARCHITECTURE

In this section, we propose two new 2-D fourfold rotational-symmetry IIR and FIR digital filter architectures. The general transfer function of a 2-D IIR digital filter can be represented as

$$H(z_1,z_2)=\frac{\sum_{i=0}^{N_1}\sum_{j=0}^{N_2}a_{i,j}z_1^{-i}z_2^{-j}}{\sum_{i=0}^{N_1}\sum_{j=0}^{N_2}b_{i,j}z_1^{-i}z_2^{-j}}=\frac{N(z_1,z_2)}{D(z_1,z_2)} \tag{4}$$

where $b_{0,0}=1$, $a_{i,j}$ as well as $b_{i,j}$ and $N_1\times N_2$ are coefficients and the order of the IIR digital filter, respectively. Throughout this paper, a square image $M\times M$ is fed to the following structures in raster-scan mode, and thus the delay $z_2^{-1}=z^{-1}$ and $z_1^{-1}=z^{-M}$, where z^{-1} and M denote a unit delay element and the width of an image, respectively. Since each $N(z_1,z_2)$ possesses fourfold rotational symmetry property discussed above for Q, we select the numerator to be $N(z_1,z_2)=N(z_2^{-1},z_1)z_2^{-N_2}$, which is the fourfold rotational symmetry condition in (3a). Here $z_2^{-N_2}$ is included to ensure the polynomial nature of $N(z_1,z_2)$. Consequently, the coefficients have to satisfy the condition of $a_{i,j}=a_{j,N_2-i}$ [5]. Besides the numerator, the denominator is chosen to be $D(z_1,z_2)=D_1(z_1)D_1(z_2)$, which is separable such that the stability can be easily assured. At the same time, the denominator also possesses fourfold rotational symmetry property. As a representative example, we perform and deduce the order of structures under an assumption $N_1=N_2=2$. The following forms for the numerator and denominator are expressed in (5a) and (5b). In (5a), it can be seen that only the boxed coefficients are independent, and the other coefficients can be obtained by rotating the boxed coefficients in steps of 90° around the mid-point of the whole matrix. Owing to the separability of the denominator, we can obtain $b_{i,j}$=$b_{j,i}$ as shown in (5b).

$$N(z_1,z_2)=\begin{matrix} & z_2^{0} & z_2^{-1} & z_2^{-2} \\ z_1^{0} & \boxed{a_{00}} & \boxed{a_{01}} & a_{00} \\ z_1^{-1} & a_{01} & \boxed{a_{11}} & a_{01} \\ z_1^{-2} & a_{00} & a_{01} & a_{00}\end{matrix} \tag{5a}$$

$$D(z_1,z_2)=\begin{matrix} & z_2^{0} & z_2^{-1} & z_2^{-2} \\ z_1^{0} & \boxed{1} & b_{01} & b_{02} \\ z_1^{-1} & \boxed{b_{01}} & \boxed{b_{11}} & b_{12} \\ z_1^{-2} & \boxed{b_{02}} & \boxed{b_{12}} & \boxed{b_{22}}\end{matrix} \tag{5b}$$

Initially, we can express (4) for $N_1=N_2=2$ as follows.

$$Y=\sum_{i=0}^{2}\sum_{j=0}^{2}a_{i,j}z_1^{-i}z_2^{-j}(X)-\sum_{i=0}^{2}\sum_{\substack{j=0\\ i+j\neq 0}}^{2}b_{i,j}z_1^{-i}z_2^{-j}(Y) \tag{6}$$

where $X=X(z_1,z_2)$ and $Y=Y(z_1,z_2)$ are defined as input and output of the digital filter, respectively. Due to the fourfold rotational symmetry property in (5a) and (5b), we recast (6) using register reordering in (7)

$$\begin{aligned}Y=&\,ka_{l,l}[z_1^{-l}z_2^{l\times P}(z_2^{-l\times P}z_2^{-l})]X-\sum_{i=1}^{2}b_{i,i}z_1^{-i}z_2^{i\times P}(z_2^{-i\times P}z_2^{-i})Y\\ &+\sum_{i=0}^{l-k}\sum_{j=0}^{l}a_{i,j}[z_1^{-i}z_2^{i\times P}(z_2^{-i\times P}z_2^{-j})+z_1^{-j}z_2^{j\times P}(z_2^{-j\times P}z_2^{-(2-i)})\\ &+z_1^{-(2-i)}z_2^{(2-i)\times P}(z_2^{-(2-i)\times P}z_2^{-(2-j)})+z_1^{-(2-j)}z_2^{(2-j)\times P}(z_2^{-(2-j)\times P}z_2^{-i})]X\\ &-\sum_{i=0}^{2}\sum_{j=i+1}^{2}b_{i,j}[z_1^{-i}z_2^{i\times P}(z_2^{-i\times P}z_2^{-j})+z_1^{-j}z_2^{j\times P}(z_2^{-j\times P}z_2^{-i})]Y\end{aligned} \tag{7}$$

Where $k=(N+1)\bmod 2$, $l=\lfloor N/2\rfloor$ for l and $a_{l,l}$, and integer variable P is restricted in range of 0 and M. Since the image is in the raster scan of this paper, the delay $z_1^{-1}=z^{-M}$ are realized by a shift-register (SR) with size of M. Thus, the terms of $z_1^{-i}z_2^{i\times P}=z_2^{-i(M-P)}$ can be implemented by the number of (*M-P*) shift registers. Next, we deduce two VLSI architectures with respect to P=0 and P=1.

◆ Type I with P=0:

Equation (7) can be expressed in (8).

$$\begin{aligned}Y=&\,ka_{l,l}(z_1^{-l}z_2^{-l})X-\sum_{i=1}^{2}b_{i,i}z_1^{-i}z_2^{-i}Y\\ &+\sum_{i=0}^{l-k}\sum_{j=0}^{l}a_{i,j}[z_1^{-i}z_2^{-j}+z_1^{-j}z_2^{-(2-i)}+z_1^{-(2-i)}z_2^{-(2-j)}+z_1^{-(2-j)}z_2^{-i}]X\\ &-\sum_{i=0}^{2}\sum_{j=i+1}^{2}b_{i,j}[z_1^{-i}z_2^{-j}+z_1^{-j}z_2^{-i}]Y\end{aligned} \tag{8}$$

Equation (8) can be mapped onto the fourfold-rotational-symmetry IIR filter architecture as depicted in Fig. 1. In addition, the users merely set $b_{i,j}$ to zero except $b_{0,0}$=1 such that a new fourfold-rotational-symmetry FIR filter architecture as shown in Fig. 2 can be obtained. In this case, although the proposed type-I IIR filter has the lowest number of multipliers, the larger critical period and global broadcast are incurred. Thus, we are motivated to derive another type filter with less critical period and local broadcast.

◆ Type II with P=1:

Observing the architectures in Fig. 1 and Fig. 2, we find that the critical period is larger and the input and output signals are globally broadcast. It is harmful to the limited fanout VLSI design. In order to enhance this architecture with higher speed and local broadcast, we set P=1 in (9).

$$\begin{aligned}Y &= ka_{l,l}[z_1^{-l} z_2^{l} (z_2^{-l} z_2^{-l})]X - \sum_{i=1}^{2} b_{i,i} z_1^{-i} z_2^{i} (z_2^{-i} z_2^{-i})Y \\ &+ \sum_{i=0}^{l-k} \sum_{j=0}^{l} a_{i,j}[z_1^{-i} z_2^{i} (z_2^{-i} z_2^{-j}) + z_1^{-j} z_2^{j} (z_2^{-j} z_2^{-(2-i)}) \\ &+ z_1^{-(2-i)} z_2^{(2-i)} (z_2^{-(2-i)} z_2^{-(2-j)}) + z_1^{-(2-j)} z_2^{(2-j)} (z_2^{-(2-j)} z_2^{-i})]X \\ &- \sum_{i=0}^{2} \sum_{j=i+1}^{2} b_{i,j}[z_1^{-i} z_2^{i} (z_2^{-i} z_2^{-j}) + z_1^{-j} z_2^{j} (z_2^{-j} z_2^{-i})]Y\end{aligned} \qquad (9)$$

In similar behaviors, the resulting fourfold-rotational-symmetry IIR architecture corresponding to (9) is shown in Fig. 3. In addition, we can also obtain a new fourfold-rotational-symmetry FIR filter architecture in Fig. 4 by setting $b_{i,j}$ to zero except $b_{0,0}$=1.

COMPARISON RESULTS OF IIR AND FIR DIGITAL FILTERS

In this section, the comprehensive comparison results of IIR and FIR filter architectures are tabulated in Table 1 and 2, respectively. The evaluation metrics are in terms of number of multipliers, critical period, latency, and local broadcast, where each critical period is calculated by tree method. Here k is the same as the definition in (7). In Table 1, it is shown that the proposed type I and type II architectures lead to the lowest number of multipliers than that of [8, 10, 11]. Among the proposed two type IIR filter architectures, the former has less number of delay elements and the latter has higher throughput and local broadcast. Analogously, we compare the performance of these FIR filters as listed in Table 2 after setting $b_{i,j}$ to zero except $b_{0,0}$=1. For the proposed second-order IIR and FIR filters, the reduction of number of multipliers can be achieved 52.9% and 66.7%, respectively. From Tables 1 and 2, we guarantee that the presented type-I structure with fourfold rotational symmetry has the lowest number of multipliers, and zero latency. Importantly, the proposed type-II IIR filter possesses high speed, local broadcast, and the same number of multipliers and latency as the type I shows at expense of a slight increment of number of delay elements.

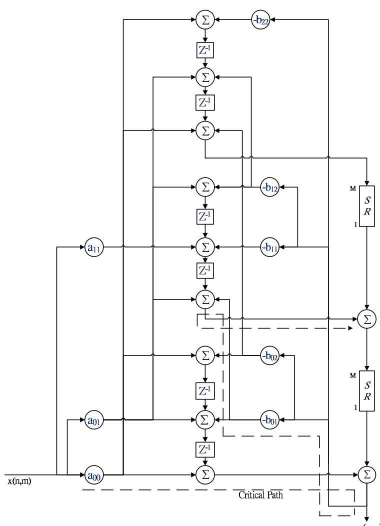

Figure 1. Proposed 2-D fourfold rotational symmetry IIR filter architecture with P=0.

V. CONCLUSION

Two new implementation of 2-D fourfold-rotational-symmetry IIR and FIR digital filter architectures have been presented. The proposed structures have the lowest number of multipliers, high throughput, and zero latency. In addition, the percentage of the reduction of number of multipliers for the proposed IIR and FIR filters are nearly 62.5% and 75%, respectively, as N is large enough.

REFERENCES

[1] A. M. Tekalp, *Digital Video Processing*. Englewood Cliffs, NJ: Prentice-Hall, 1995, chap 14.

[2] M. A. Sid-Ahmed, Image Processi*ng: Theory, Algorithms, and Architectures*. NY: McGraw-Hill, 1995.

[3] D. E. Dudgeon and R. M. Mersereau, *Multidimensional Digital Signal Processing.* Englewood Cliffs, NJ: Prentice-Hall, 1984, Chap 4.

[4] H. Mohammadzade, L. T. Bruton,, "A simultaneous div-curl 2D Clifford Fourier Transform filter for enhancing vortices, sinks and sources in sampled 2D vector field images," in *Proc. IEEE International Symposium on Circuits and Systems*, May. 2007, pp. 821-824.

[5] H. C. Reddy, I. H. Khoo, P. K. Rajan, "2-D symmetry: theory and filter design applications," *IEEE Circuits and Systems Magazine,* vol. 3, pp. 4-33, 2003.

[6] M. N. S. Swamy and P. K. Rajan, "Symmetry in 2-D filters and its application," in *Multidimensional Systems: Techniques and Applications* (S.G. Tzafestas, Ed.). New York: Marcel Dekkar, 1986, Ch.9.

[7] S. K. Mitra, A. D. Sagar, and N. A. Pendergrass, " Realization of two-demensinal recursive digital filters," *IEEE Trans. Circuits Syst*., vol. 22, pp. 171-184, Mar. 1975.

[8] S. Chakrabarti and S. K. Mitra, "Decision methods and realization of 2-D digital filters using minimum number of delay elements," *IEEE Trans. Circuits Syst*., vol. 27, pp. 657-666, Aug. 1980.

[9] M. A. Sid-Ahmed, "A systolic realization for 2-D digital filters," *IEEE Trans. Acoust., Speech, Signal Processing*, vol. ASSP-37, pp. 560-565, Apr. 1989

[10] S. Sunder, F. El-Guibaly, and A. Antoniou, "Systolic implementations of two-dimensional recursive digital filters," in *Proc. IEEE Int. Symp. Circuits Syst.*, May 1990, pp. 1034-1037.

[11] L. D. Van, "A new 2-D systolic digital filter architecture without global broadcast," *IEEE Trans. VLSI syst.,* vol. 10, no. 4, pp. 477-486, Aug. 2002

[12] P. Y. Chen, L. D. Van, H. C. Reddy and C.T. Lin, "A new VLSI 2-D diagonal-symmetry filter architecture design," in *Proc. IEEE APCCAS,* Dec. 2008, Macao, China, accepted.

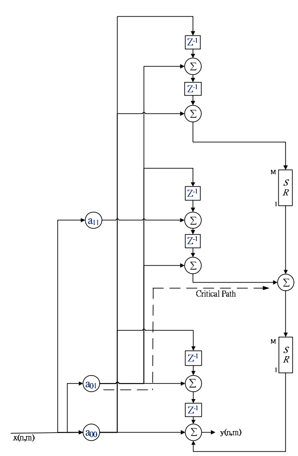

Figure 2. Proposed 2-D fourfold-rotational-symmetry FIR filter architecture with P=0.

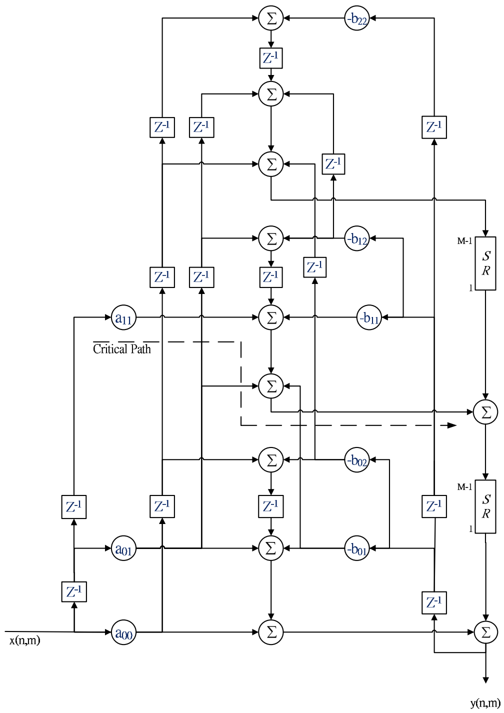

Figure 3. Proposed 2-D fourfold-rotational-symmetry IIR filter architecture with *P*=1.

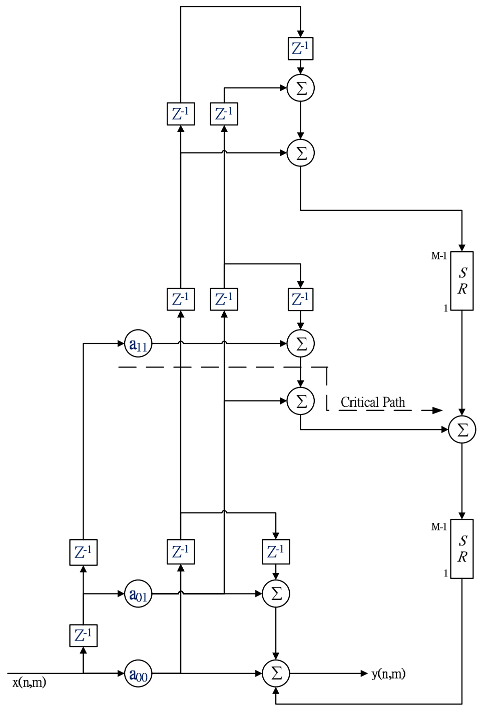

Figure 4. Proposed 2-D fourfold-rotational-symmetry FIR filter architecture with *P*=1.

Table 1 Comparison Results among the IIR Digital Filter Architecture

Parameter	Ahmed [8]	Van [10]	Chen with *P*=1 [11]	This Work with *P*=0	This Work with *P*=1
No. of Multipliers	$2(N+1)^2-1$	$2(N+1)^2-1$	$(N+1)^2+N$	$\frac{3}{4}(N+1)^2+\frac{1}{2}N+\frac{3}{4}k-\frac{1}{2}$	$\frac{3}{4}(N+1)^2+\frac{1}{2}N+\frac{3}{4}k-\frac{1}{2}$
Critical Period	$T_m+(2+\lceil \log_2(N+1)\rceil)T_a$	T_m+3T_a	T_m+3T_a	$2T_m+2T_a$	T_m+3T_a
Latency	1	0	0	0	0
Local Broadcast	No	Yes	Yes	No	Yes

Table 2 Comparison Results among the FIR Digital Filter Architecture

Parameter	Ahmed [8]	Van [10]	Chen with *P*=1 [11]	This Work with *P*=0	This Work with *P*=1
No. of Multipliers	$(N+1)^2$	$(N+1)^2$	$\frac{(N+1)^2+N+1}{2}$	$\frac{1}{4}(N+1)^2+\frac{3}{4}k$	$\frac{1}{4}(N+1)^2+\frac{3}{4}k$
Critical Period	$\max\{(T_m+T_a), (\lceil \log_2(N+1)\rceil)T_a\}$	T_m+2T_a	T_m+2T_a	T_m+T_a	T_m+2T_a
Latency	1	0	0	0	0
Local Broadcast	No	Yes	Yes	No	Yes